Effects of angular dependence of surface diffuseness in deformed nuclei on Coulomb barrier

G. G. Adamian, N. V. Antonenko, and L. A. Malov
Joint Institute for Nuclear Research, 141980 Dubna, Russia

G. Scamps
GANIL, CEA/DSM and CNRS/IN2P3, Boîte Postale 55027, 14076 Caen Cedex, France

D. Lacroix
Institut de Physique Nucléaire, IN2P3-CNRS, Université Paris-Sud, F-91406 Orsay Cedex, France
(Received 16 August 2014; published 30 September 2014)

The angular dependence of surface diffuseness is further discussed. The results of self-consistent calculations are compared with those obtained with the phenomenological mean-field potential. The rather simple parametrizations are suggested. The effects of surface polarization and hexadecapole deformation on the height of the Coulomb barrier are revealed.

DOI: 10.1103/PhysRevC.90.034322 PACS number(s): 21.10.Ft, 21.60.Jz, 27.70.+q, 27.90.+b

I. INTRODUCTION

The study of nucleon distribution in atomic nuclei is expected to provide valuable information for the understanding of nuclear excitations, the appearance of the new magic numbers near the drip lines, and the difference between proton and neutron nuclear radii to study the symmetry energy [1–9]. The surface diffuseness correction is necessary to improve the accuracy of the macroscopic-microscopic mass formula for unstable nuclei [10]. The surface effect of the symmetry potential plays an important role in the nuclei near the drip lines. The nucleon density profile affects the nucleus-nucleus interactions as well. It is important for the determination of the fusion barrier between two colliding nuclei.

The self-consistent methods provide us the ground-state deformations that depend on the specific interaction used in the energy-density functional [11,12]. The nucleus-nucleus potential is usually sensitive to the deformations of nuclei as well as to their surface diffuseness. Usually the predictions of quadrupole deformations vary within 20% and the predicted values of hexadecapole deformations vary much more [11]. Rather large uncertainty in the values of hexadecapole deformation parameters β_4 would create an uncertainty in the barrier of the nucleus-nucleus potential that has to be studied.

In Ref. [13], we have revealed the angle dependence of the surface diffuseness in deformed nuclei observed within self-consistent calculations. The energy-density functional based on Skyrme effective interaction was used to study the nucleon distributions in the nuclear ground states. In the present article, we discuss further the angular dependence of surface diffuseness induced by deformation and provide useful expressions for this dependence (Sec. II). The role of polarization of the diffuseness in the symmetry energy is also discussed. In Sec. III the isotopic dependence of the surface diffuseness is studied. The role of hexadecapole deformation in the nucleus-nucleus interaction potential is treated as well and provided by analytical expressions in Sec. IV and the Appendix. The conclusions are given in Sec. V.

II. ANGULAR DEPENDENCE OF SURFACE DIFFUSENESS

In well-deformed nuclei ($\beta_2 \geqslant 0.2$) the diffuseness along the symmetry axis ($\theta = 0$) seems to be smaller than that along the axis perpendicular to the symmetry axis ($\theta = \pi/2$). This effect can be seen in Fig. 1, where the density is computed using the EV8 code [14] with the Sly6 [15] interaction. At $\theta = 0$ the nucleon density distribution has a maximum near the surface. After this maximum (Fig. 1) ρ steeply falls with increasing R. At $\theta = \pi/2$ the value of ρ has no maxima near the nuclear surface and decreases slower with increasing R. For weakly deformed nuclei, the diffuseness is slightly larger at $\theta = 0$ than at $\theta = \pi/2$. In Fig. 2 we show the difference of diffuseness a_L along the long axis and diffuseness a_S along the short axis for the deformed nuclei with $\beta_2 \geqslant 0.2$. While the nuclei with $A = 120$–140 and 150–190 the difference of a_L and a_S is about 5%, it is about two times larger in the nuclei with $A = 230$–260. So, the effects of angular dependence of the diffuseness are expected to be more pronounced especially in the actinide region.

A limitation of the self-consistent method is that it is not possible to change the deformation parameters. In consequence a simpler model is used here. We impose the mean-field potential as the Woods-Saxon potential with spin-orbit interaction and solve the Schrödinger equation in it [16], then we can look at the nucleon density profile at different values of quadrupole and hexadecapole deformations and directly get phenomenological insight of their effects. The density profiles obtained would have more oscillations than in Fig. 1 because the pairing is not taken into account in this case. The maximum of $\rho(R)$ near the surface is well seen at $\theta = 0$ (Figs. 3 and 4). After this maximum ρ steeply decreases and the diffuseness is smaller at $\theta = 0$. Naively, one can expect larger diffuseness at $\theta = 0$ because stiffness of the single-particle potential is smaller along the long nuclear semiaxis and the nucleons spend more time near the surface. Indeed, the nucleons spend more time closer to the nuclear surface that provides the maximum in $\rho(R)$ near the surface. However, after the resulted maximum of nucleon density the diffuseness becomes smaller. This feature is better seen for larger deformed nuclei like ^{152}Sm in Fig. 4.

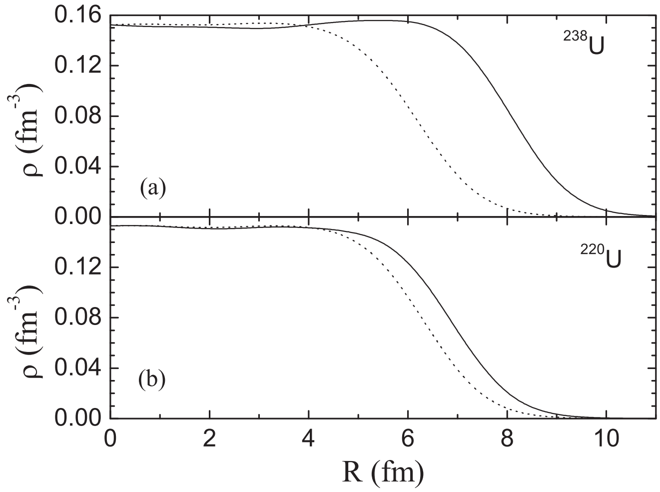

FIG. 1. The calculated nucleon density distributions along the symmetry axis at $\theta = 0$ (solid lines) and along the perpendicular axis at $\theta = \pi/2$ (dotted lines) in well-deformed ^{238}U (a) and in weakly deformed ^{220}U (b).

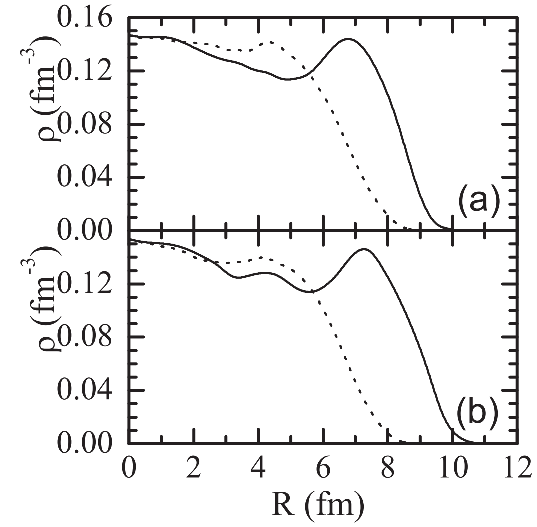

FIG. 3. The calculated nucleon density distributions along the symmetry axis at $\theta = 0$ (solid lines) and along the perpendicular axis at $\theta = \pi/2$ (dotted lines) in ^{238}U. The deformation parameters are $\beta_2 = 0.254$ and $\beta_4 = 0$ (a) and $\beta_2 = 0.254$ and $\beta_4 = 0.08$ (b).

From the nucleon density that resulted from the Woods-Saxon potential one can see whether the hexadecapole deformation affects the angular dependence of diffuseness. In Fig. 3, the nucleon density profiles are shown at $\theta = 0$ and $\pi/2$ for ^{238}U at $\beta_2 = 0.254$ with $\beta_4 = 0$ and $\beta_4 = 0.08$. As seen, the hexadecapole deformation does only marginally affect the angular dependence of the diffuseness.

In Fig. 5, the diffuseness of the nucleon density distribution in ^{238}U is depicted as a function of angle with respect to the symmetry axis. The calculations were performed with SLy6 and SLy4 forces. The dependencies of a on θ are similar in two cases and can be approximated for actinides at $0 \leqslant \theta \leqslant \pi/2$ as follows:

$$a(\theta) = a(0) + 0.45 \sin^2 \theta - 0.4 \sin^3 \theta.$$

For the region of rare-earth nuclei, the same functional dependence is valid, but with different coefficients:

$$a(\theta) = a(0) + 0.25 \sin^2 \theta - 0.25 \sin^3 \theta.$$

In the mass formula, the symmetry energy $\sim \int d\mathbf{r}[\rho_n(\mathbf{r}) - \rho_p(\mathbf{r})]/[\rho_n(\mathbf{r}) + \rho_p(\mathbf{r})]$ depends on the difference of the neutron and proton density profiles. The surface region is built by quite different proton and neutron orbitals. However, the angular dependencies of proton and neutron diffuseness are similar and ruled by the deformed mean field. As follows from our coarse estimate, the symmetry energy changes up to a few hundred keV due to the angular dependence of diffusion. So, the angular dependence of the diffuseness could result in some low-lying excited states in nuclei.

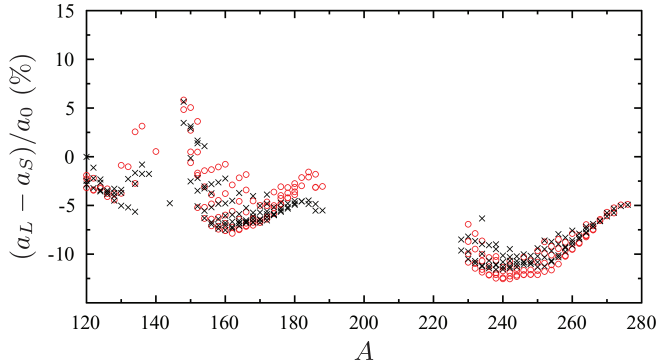

FIG. 2. (Color online) The value of $(a_L - a_S)/a_0$ as a function of mass in %. a_0 is an average diffuseness. The black crosses and red open circles correspond, respectively, to results obtained with the SkM* and Sly4 functionals.

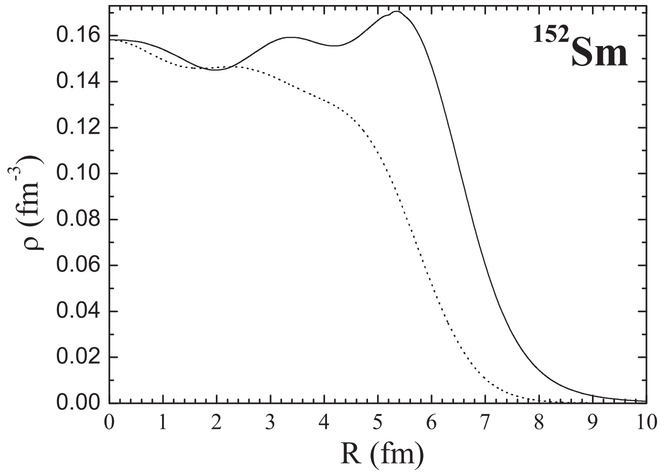

FIG. 4. The calculated nucleon density distributions along the symmetry axis at $\theta = 0$ (solid lines) and along the perpendicular axis at $\theta = \pi/2$ (dotted lines) in ^{152}Sm. The deformation parameters are $\beta_2 = 0.27$ and $\beta_4 = 0.1$.

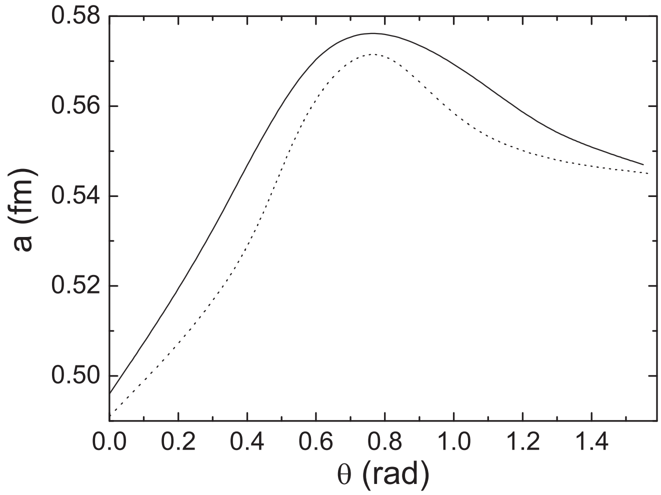

FIG. 5. The calculated dependence of nucleon density distribution diffuseness for ^{238}U on the angle with respect to the symmetry axis. The results obtained with SLy6 and SLy4 forces are presented by dotted and solid lines, respectively.

III. ISOTOPIC DEPENDENCE OF SURFACE DIFFUSENESS

For well-deformed even-even isotopes $^{226-240}$U, the values of diffuseness at $\theta = 0$, $\pi/4$, and $\pi/2$ are depicted in Fig. 6 as a function of $x = \sqrt{5.93/S_n}$. Here, S_n is the experimental neutron separation energy and $S_n = 5.93$ MeV in ^{240}U. One can see that $a(x)$ can be roughly approximated at each θ by linear function:

$$a(x) \approx a(x = 1) + \xi(x - 1), \tag{1}$$

where $\xi = 0.12$–0.14 for nuclei treated. The value of a increases by about 2–4% with increasing mass number by about 6%. Note that in Ref. [17] the simpler linear dependence $a(x) = a(x = 1)x$ was used.

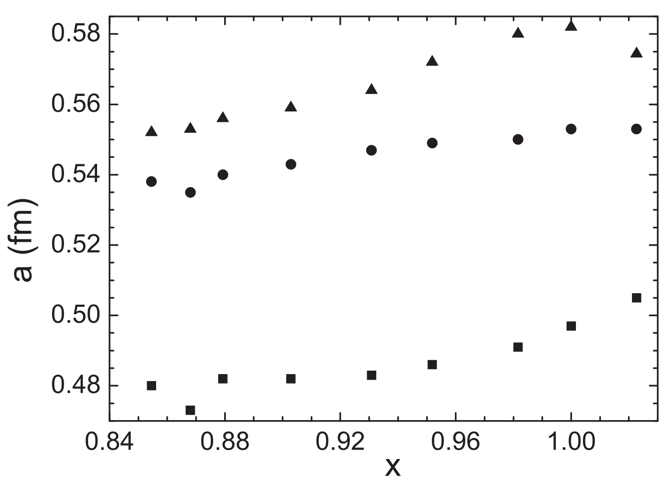

FIG. 6. The calculated isotopic dependencies of nucleon density distribution diffuseness on $x = \sqrt{5.93/S_n}$, where S_n is the experimental neutron separation energy, at angles $\theta = 0$ (squares), $\pi/4$ (circles), and $\pi/2$ (triangles) for even-even isotopes $^{226-240}$U.

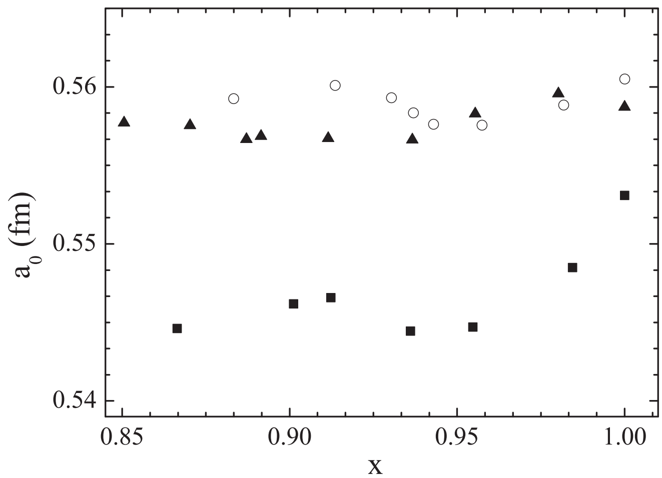

FIG. 7. The calculated isotopic dependencies of average diffuseness on $x = \sqrt{S_n'/S_n}$, where S_n is the experimental neutron separation energy. For $^{220-234}$Ra (open circles), $^{220-238}$Th (triangles), and $^{240-252}$Cm (squares) even isotopes, the values S_n' equal to S_n in ^{234}Ra, ^{238}Th, and ^{252}Cm, respectively.

The deviation from linear dependence occurs at x corresponding to the neutron subshell at $N = 150$–152. The diffuseness becomes smaller by a few percent in actinides with $N = 150$–152 in comparison with the neighboring isotopes. However, Eq. (1) is still useful for rough estimates. As found, it is also suitable for the isotopic dependence of average value of diffuseness defined as

$$a_0 = \int_0^{\pi/2} a(\theta) \sin\theta d\theta. \tag{2}$$

As seen in Fig. 7, the dependencies of $a_0(x)$ are rather close to the linear ones.

IV. THE COULOMB BARRIER

To calculate the nucleus-nucleus interaction potential $V(R)$, we use the procedure presented in Refs. [18,19]. The nucleus-nucleus interaction potential at zero angular momentum ($L = 0$) is given as

$$V(R) = V_N(R) + V_C(R). \tag{3}$$

For the nuclear part of the nucleus-nucleus potential, the double-folding formalism with density-dependent effective nucleon-nucleon interaction is used. Within this approach many heavy-ion capture reactions with stable and radioactive beams at energies above and well below the Coulomb barrier have been successfully described [20]. The quadrupole deformations of colliding nuclei are taken into consideration in this approach. Here, we take into account only the quadrupole $[\beta_2^{(i)}]$ and hexadecapole $[\beta_4^{(i)}]$ deformations ($i = 1,2$).

For the Coulomb barrier one can obtain the relationships between the derivatives of V_N and V_C:

$$\left(\frac{dV}{dR}\right)_{R=R_b} = 0, \tag{4}$$

$$\left(\frac{dV_N}{dR}\right)_{R=R_b} = -\left(\frac{dV_C}{dR}\right)_{R=R_b} = \frac{Z_1Z_2e^2}{R_b^2}, \tag{5}$$

and

$$\left(\frac{d^2V}{dR^2}\right)_{R=R_b} = -\mu\omega_b^2, \tag{6}$$

$$\left(\frac{d^2V_N}{dR^2}\right)_{R=R_b} = -\mu\omega_b^2 - \left(\frac{d^2V_C}{dR^2}\right)_{R=R_b} = -\mu\omega_b^2 - \frac{2Z_1Z_2e^2}{R_b^3}. \tag{7}$$

Here, R_b and ω_b are the position and the frequency, respectively, of the Coulomb barrier for the spherical nuclei at $L = 0$. The $\mu = m_0A_1A_2/(A_1 + A_2)$ is the reduced mass parameter with the nucleon mass m_0 and the Z_i (A_i) is the atomic (mass) number of nucleus i. The exact formula for the Coulomb nucleus-nucleus interaction is

$$V_C = \frac{Z_1Z_2e^2}{R} + \left(\frac{9}{20\pi}\right)^{1/2}\frac{Z_1Z_2e^2}{R^3}\sum_{i=1,2}R_i^2\beta_2^{(i)}\left[1+\frac{2}{7}\left(\frac{5}{\pi}\right)^{1/2}\beta_2^{(i)}\right]P_2(\cos\theta_i) + \left(\frac{1}{4\pi}\right)^{1/2}\frac{Z_1Z_2e^2}{R^5}\sum_{i=1,2}R_i^4\beta_4^{(i)}P_4(\cos\theta_i). \tag{8}$$

This expression is for interacting two deformed nuclei with sharp charge distributions. The diffuseness is known [21] and can be disregarded in the calculation of V_C. Equation (8) is well tested at R near R_b. Note that at $R \approx R_b$ the overlap of nucleon-density tails is rather small to be taken into account.

One can expand the nuclear part V_N of the nucleus-nucleus interaction around $R = R_b$ as follows:

$$V_N = V_N^{\rm sp}(R_b) - \left(\frac{dV_N}{dR}\right)_{R=R_b}\Delta R + \frac{1}{2}\left(\frac{d^2V_N}{dR^2}\right)_{R=R_b}(\Delta R)^2, \tag{9}$$

$$\Delta R = \left(\frac{5}{4\pi}\right)^{1/2}\sum_{i=1,2}R_i\beta_2^{(i)}P_2(\cos\theta_i) + \left(\frac{9}{4\pi}\right)^{1/2}\sum_{i=1,2}R_i\beta_4^{(i)}P_4(\cos\theta_i). \tag{10}$$

Using Eqs. (3), (5), (7), and (8), we obtain

$$\begin{aligned} V_N = {}& V_N^{\rm sp}(R_b) - \left(\frac{5}{4\pi}\right)^{1/2}\frac{Z_1Z_2e^2}{R_b^2}\sum_{i=1,2}R_i\beta_2^{(i)}P_2(\cos\theta_i) + \frac{5}{8\pi}\left(-\mu\omega^2 - \frac{2Z_1Z_2e^2}{R_b^3}\right)\sum_{i=1,2}\left[R_i\beta_2^{(i)}P_2(\cos\theta_i)\right]^2 \\ & + \frac{5}{4\pi}\left(-\mu\omega^2 - \frac{2Z_1Z_2e^2}{R_b^3}\right)R_1R_2\beta_2^{(1)}\beta_2^{(2)}P_2(\cos\theta_1)P_2(\cos\theta_2) - \left(\frac{9}{4\pi}\right)^{1/2}\frac{Z_1Z_2e^2}{R_b^2}\sum_{i=1,2}R_i\beta_4^{(i)}P_4(\cos\theta_i), \end{aligned} \tag{11}$$

where $V_N^{\rm sp}$ is the nuclear part of the nucleus-nucleus interaction for the spherical nuclei. By summing V_C from Eq. (7) and V_N from Eq. (10), we obtain that the Coulomb barrier has the following dependence on the orientations of the deformed nuclei [the change of the Coulomb interaction up to $(\beta_2^{(i)})^2$ and nuclear interaction with orientations up to $(\beta_2^{(i)})^2$]:

$$\begin{aligned} V_b(\theta_i) = {}& V_b^{\rm sp} + \sum_{i=1,2}f_i\big(R_b,\beta_2^{(i)}\big)\beta_2^{(i)}P_2(\cos\theta_i) + \sum_{i=1,2}g_i(R_b)\big[\beta_2^{(i)}P_2(\cos\theta_i)\big]^2 + h_0(R_b)\beta_2^{(1)}\beta_2^{(2)}P_2(\cos\theta_1)P_2(\cos\theta_2) \\ & + \sum_{i=1,2}k_i(R_b)\beta_4^{(i)}P_4(\cos\theta_i), \end{aligned} \tag{12}$$

where $V_b^{\rm sp} = V_N^{\rm sp}(R_b) + Z_1Z_2e^2/R_b$ and

$$f_i\big(R_b,\beta_2^{(i)}\big) = \frac{1}{(20\pi)^{1/2}}\frac{Z_1Z_2e^2R_i}{R_b^2}\left[-5 + \frac{3R_i}{R_b}\left(1+\frac{2}{7}\left(\frac{5}{\pi}\right)^{1/2}\beta_2^{(i)}\right)\right], \tag{13}$$

$$g_i(R_b) = \frac{5R_i^2}{8\pi}\left[-\mu\omega_b^2 - \frac{2Z_1Z_2e^2}{R_b^3}\right], \tag{14}$$

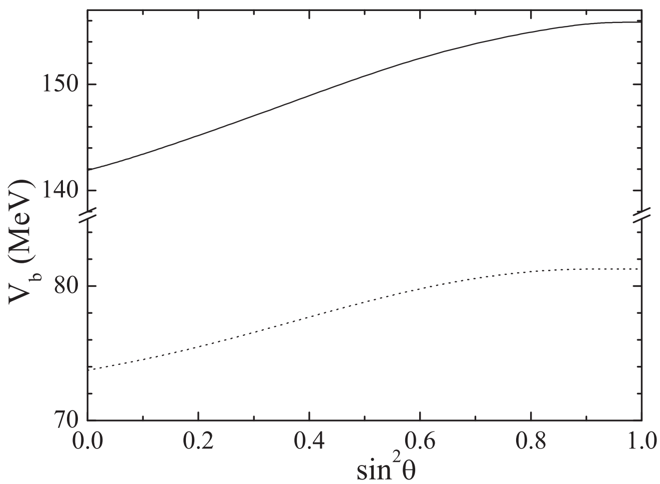

FIG. 8. The calculated dependencies of the Coulomb-barrier heights V_b on the orientation angle θ in the reactions ${}^{36}S + {}^{238}U$ (solid line) and ${}^{16}O + {}^{238}U$ (dotted line). The result obtained with nucleon density distributions calculated for ${}^{238}U$ with the Hartree-Fock-Bogoliubov approach.

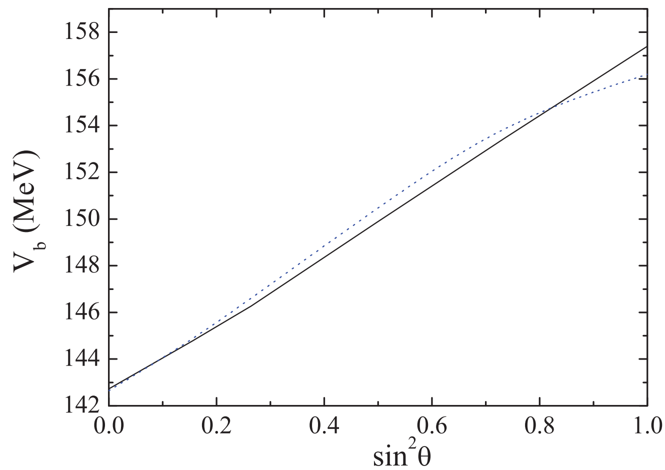

FIG. 9. (Color online) The calculated dependencies of the Coulomb-barrier heights V_b on the orientation angle θ in the ${}^{36}S + {}^{238}U$ reaction. The results obtained with $a = 0.56$ fm, $\beta_2 = 0.286$, and $\beta_4 = 0$ for ${}^{238}U$ are presented by solid line. The dotted line corresponds to $a(\theta)$, $\beta_2 = 0.244$, and $\beta_4 = 0.08$. For ${}^{36}S$, the diffuseness parameter is 0.55 fm.

$$h_0(R_b) = \frac{5R_1R_2}{4\pi}\left[-\mu\omega_b^2 - \frac{2Z_1Z_2e^2}{R_b^3}\right], \tag{15}$$

$$k_i(R_b) = \frac{1}{(4\pi)^{1/2}}\frac{Z_1Z_2e^2R_i}{R_b^2}\left[-3 + \frac{R_i^3}{R_b^3}\right]. \tag{16}$$

The main inputs in the calculation of $V(R)$ are the parameters of radius r_0 and diffuseness a. The barrier height V_b does not depend on a explicitly but through the values of R_b and ω_b. Here, we set $r_0 = 1.15$ fm and look at the dependence of the fusion barrier on $a(\theta_2) = a(\theta)$ and deformation parameters. We consider the reactions ${}^{36}S + {}^{238}U$ and ${}^{16}O + {}^{238}U$ with spherical light nuclei and deformed heavy nucleus. It is interesting to understand why in the calculations with constant diffuseness and only quadrupole deformation one can successfully describe the experimental data. In the phenomenological calculation of the nucleus-nucleus potential the hexadecapole deformations of interacting nuclei are often disregarded. The direct calculations of the Coulomb barrier heights with $a(\theta)$, $\beta_2^{(2)} = \beta_2 = 0.244$ ($\beta_2^{(1)} = 0$), and $\beta_4^{(2)} = \beta_4 = 0.094$ ($\beta_4^{(1)} = 0$) demonstrate almost linear dependence of V_b on $\sin^2\theta$ (Fig. 8). As found, the angular dependence of a causes small deviations from the linear dependence.

Employing the Eqs. (12) and (A7) (see the Appendix) for $V_b(\theta)$ and numerical calculations of the nucleus-nucleus interaction potential, one can suggest a simple approximation of the Coulomb barrier height:

$$V_b(\theta) = V_b(0) + \alpha\frac{Z_1Z_2A_2^{1/3}}{\left(A_1^{1/3} + A_2^{1/3}\right)^2}(\beta_2 + f\beta_4)\sin^2\theta, \tag{17}$$

where $\alpha \approx 0.50$ and $f \approx 0.81$ for the reactions considered. As seen, almost the same values of $V_b(\theta)$ can be obtained with $\beta_4 \neq 0$ and $\beta_4 = 0$ by properly varying β_2. This is illustrated in Fig. 9. Taking the experimental $\beta_2 = 0.286$ for ${}^{238}U$, we calculate $V_b(\theta)$ at constant diffuseness $a = 0.56$ fm for ${}^{238}U$ in the ${}^{36}S + {}^{238}U$ reaction. Using the fact that $a(\theta)$ weakly depends on β_4, we show that almost the same results can be obtained with $a(\theta)$, $\beta_2 = 0.244$, and $\beta_4 = 0.08$. Note that in ${}^{238}U$ we have $a_0 = 0.55$ fm.

In many applications the phenomenological calculation of the Coulomb barrier performed with only β_2 and constant average diffuseness results in almost the same value as in the consistent calculations with β_4 and $a(\theta)$ because the disregard of β_4 in the calculation of V_b can be negated by the proper change of β_2 at constant diffuseness. This is why the phenomenological calculations are successful to describe the experimental data.

The average values of the Coulomb barrier V_b are defined as

$$\bar{V}_b = \int_0^{\pi/2} V_b(\theta)\sin\theta d\theta. \tag{18}$$

We found that almost the same $\bar{V}_b$ are obtained with $a(\theta)$, $\beta_2 = 0.244$, and $\beta_4 = 0.094$ ($\bar{V}_b = 152.5$ MeV), which follow from the self-consistent treatment, and with $a = 0.56$ fm, $\beta_2 = 0.286$, and $\beta_4 = 0$ ($\bar{V}_b = 152.4$ MeV). Therefore, the processes above the Coulomb barrier are insensitive to the angular dependence of the diffuseness and the value of β_4.

V. SUMMARY

We found that the angular dependence of diffuseness is caused by the mean-field effects that create inhomogeneities on the nuclear surface. The residual interaction partly washes out these inhomogeneities. In the region of actinides the surface polarization is about two times stronger than that in the rare-earth nuclei. The angular dependence of a can be roughly approximated by the polynomial of $\sin\theta$. The isotopic dependence of the diffuseness on $1/\sqrt{S_n}$ is found to be almost linear. The deviation from the linear dependence occurs when the neutron number becomes magic or quasimagic. The simple parametrization was suggested for the height of the Coulomb barrier in the case of interacting deformed nuclei. Almost the same height of the barrier can be obtained with $\beta_4 \neq 0$ and $\beta_4 = 0$. In the last case the parameter of quadrupole deformation has to be taken to be larger. In the collisions of deformed and spherical nuclei, the barrier height is the almost linear function of $\sin^2\theta$.

ACKNOWLEDGMENTS

This work was supported by RFBR. The IN2P3(France)-JINR(Dubna) Cooperation Programme is gratefully acknowledged.

APPENDIX

For the Coulomb barrier at given orientations θ_i ($i = 1,2$) of interacting nuclei, one can obtain the following relationships:

$$\left(\frac{dV}{dR}\right)_{R=R_b(\theta_i)} = 0, \tag{A1}$$

$$\left(\frac{dV_N}{dR}\right)_{R=R_b(\theta_i)} = -\left(\frac{dV_C}{dR}\right)_{R=R_b(\theta_i)} = \frac{Z_1Z_2e^2}{R_b^2(\theta_i)}. \tag{A2}$$

Near the Coulomb barrier positions $R_b(\theta_i)$ the nuclear part of the nucleus-nucleus interaction potential can be approximated by the exponential function,

$$V_N \approx V_N^0 \exp\{-[R - R_b(\theta_i)]/a(\theta_i)\}. \tag{A3}$$

From Eqs. (A2) and (A3) one can derive the following expression for the barrier height $V_b(\theta_i)$:

$$V_b(\theta_i) = \frac{Z_1Z_2e^2}{R_b(\theta_i)}\left[1 - \frac{a(\theta_i)}{R_b(\theta_i)}\right]. \tag{A4}$$

Expanding $R_b(\theta_i)$ and $a(\theta_i)$ around $R_b(0)$ and $a(0)$, respectively,

$$R_b(\theta_i) = R_b(0) + \Delta R_b(\theta_i), \tag{A5}$$

$$a(\theta_i) = a(0) + \Delta a(\theta_i), \tag{A6}$$

and substituting Eqs. (A5) and (A6) in Eq. (A4), we finally obtain

$$V_b(\theta_i) \approx V_b(0) - \frac{Z_1Z_2e^2}{R_b^2(0)}[\Delta R_b(\theta_i) + \Delta a(\theta_i)]. \tag{A7}$$

As found from Eq. (A7), the angular dependencies of $a(\theta_i)$ and $R_b(\theta_i)$ cause the deviations of $V_b(\theta_i)$ from $V_b(0)$. Note that these two contributions have different signs. Because $\Delta R_b(\theta_i) \gg \Delta a(\theta_i)$, the main deviations come from the $\Delta R_b(\theta_i)$ term. This conclusion was proved by the numerical calculations (see main text).

Because

$$\left(\frac{d^2V_N}{dR^2}\right)_{R=R_b(\theta_i)} = \frac{1}{a(\theta)}V_N, \tag{A8}$$

one can determine the barrier stiffness:

$$\begin{aligned}\mu\omega_b^2(\theta) &= \frac{Z_1Z_2e^2[R_b(\theta_i) - 2a(\theta_i)]}{R_b^3(\theta_i)a(\theta_i)}\\ &\approx \mu\omega_b^2(0) - \frac{Z_1Z_2e^2}{R_b^3(0)a^2(0)}[2a(0)\Delta R_b(\theta_i)\\ &\quad + R_b(0)\Delta a(\theta_i)].\end{aligned} \tag{A9}$$

As seen from this equation, the angular dependence of stiffness occurs from the angular dependencies of the barrier position and the diffuseness. Because $2a(0)|\Delta R_b(\theta_i)| > R_b(0)\Delta a(\theta_i)$, $\Delta R_b(\theta_i)$ is negative and its absolute value grows with increasing θ_i, the value of stiffness for the pole-pole configuration is smaller than that for the side-side configuration.

[1] X. Viñas, M. Centelles, X. Roca-Maza, and M. Warda, AIP Conf. Proc. **1491**, 101 (2012).
[2] R. Kanungo *et al.*, Phys. Rev. C **84**, 061304 (2011).
[3] R. Kanungo *et al.*, Phys. Rev. C **83**, 021302 (2011).
[4] L.-W. Chen, C. M. Ko, and B.-A. Li, Phys. Rev. C **72**, 064309 (2005).
[5] C. J. Horowitz and J. Piekarewicz, Phys. Rev. Lett. **86**, 5647 (2001).
[6] M. Bender, G. F. Bertsch, and P.-H. Heenen, Phys. Rev. C **73**, 034322 (2006).
[7] N. Tsoneva and H. Lenske, Phys. Rev. C **77**, 024321 (2008).
[8] J.-P. Delaroche, M. Girod, J. Libert, H. Goutte, S. Hilaire, S. Péru, N. Pillet, and G. F. Bertsch, Phys. Rev. C **81**, 014303 (2010).
[9] M. Bender, P.-H. Heenen, and P.-G. Reinhard, Rev. Mod. Phys. **75**, 121 (2003).
[10] N. Wang, M. Liu, X. Wu, and J. Meng, Phys. Lett. B **734**, 215 (2014).
[11] http://www.astro.ulb.ac.be/bruslib/.
[12] B. N. Lu, E. G. Zhao, and S. G. Zhou, Phys. Rev. C **85**, 011301(R) (2012).
[13] G. Scamps, D. Lacroix, G. G. Adamian, and N. V. Antonenko, Phys. Rev. C **88**, 064327 (2013).
[14] P. Bonche, H. Flocard, and P.-H. Heenen, Comput. Phys. Commun. **171**, 49 (2005).
[15] E. Chabanat, P. Bonche, P. Haensel *et al.*, Nucl. Phys. A **635**, 231 (1998).
[16] F. A. Gareev, S. P. Ivanova, L. A. Malov, and V. G. Soloviev, Nucl. Phys. A **171**, 134 (1971).
[17] T. M. Shneidman, G. G. Adamian, N. V. Antonenko, R. V. Jolos, and W. Scheid, Phys. Rev. C **67**, 014313 (2003).
[18] V. V. Sargsyan, G. G. Adamian, N. V. Antonenko, and W. Scheid, Eur. Phys. J. A **45**, 125 (2010).
[19] V. V. Sargsyan, G. G. Adamian, N. V. Antonenko, W. Scheid, and H. Q. Zhang, Phys. Rev. C **84**, 064614 (2011).
[20] V. V. Sargsyan, G. G. Adamian, N. V. Antonenko, W. Scheid, and H. Q. Zhang, Phys. Rev. C **86**, 034614 (2012).
[21] H. J. Krappe, Ann. Phys. (N. Y.) **99**, 142 (1976).